



Porous polymer film formation by water droplet templating using polystyrene

P. V. Swathi and V. Madhurima^a

Department of Physics, School of Basic and Applied Sciences, Central University of Tamil Nadu, Thiruvavur, Tamil Nadu 610005, India

Received 8 December 2022 / Accepted 20 March 2023 / Published online 1 April 2023
© The Author(s), under exclusive licence to EDP Sciences, SIF and Springer-Verlag GmbH Germany, part of Springer Nature 2023

Abstract Studies show that the formation of breath figures over polystyrene is not clearly understood—sometimes the patterns are regular and sometimes they are barely formed. In an attempt to understand this process a little more, breath figures over polystyrene of three molecular weights and on the smooth and grooved DVD surfaces are prepared and studied. The microporous films are prepared by the evaporation of the chloroform solution of the polymers in a humid environment. The thus formed breath figure patterns are studied under a confocal laser scanning microscope and the images are analyzed. Breath figures were formed for (a) three molecular weights of the polymer (b) two casting techniques, and (c) on smooth and grooved surfaces (of a commercial DVD). The wetting of the breath figures formed by water is also reported here. The pore diameters were found to increase with increase in molecular weight and also with concentration of the polymer used. Only drop-casting method yield breath figures. Voronoi entropy, calculated from the images, indicates ordered pores on the grooved surface compared to smooth surfaces. Contact angle studies indicate a hydrophobic nature of the polymer, with the hydrophobicity increasing by the patterning.

1 Introduction

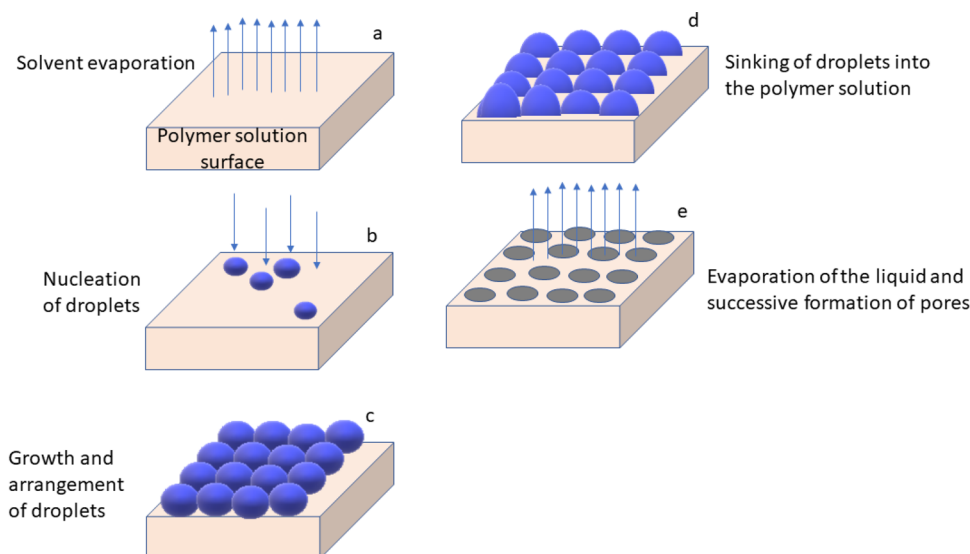
Porous polymer films have a variety of applications as catalysts [1, 2], separation and adsorbent media [3, 4], chromatographic materials [5], etc. Hence, fabricating them in a simple and controlled manner, with size scalability is of interest. A simple, cost-effective, single-stage method for the fabrication of porous polymer films is breath figure (BF) approach, which was first developed by Francois et al. [6] BF patterns are formed by the condensation of water droplets and their successive evaporation during the solidification of the polymer solution. The preparation steps consist of casting of a polymer solution on a substrate followed by controlled evaporation of solvent in a humid environment. Evaporation of solvent leads to cooling of the substrate/polymer, enabling the condensation of water droplets on the polymer surface and their successive evaporation results in the formation of pores. The schematic diagram of the steps involved in BF formation is shown in Fig. 1.

Previous studies on the formation of BFs over polystyrene (PS) indicate difficulties in analyzing them, largely because there are conflicting experimental results. A variety of parameters such as type and architecture of the polymer used, solvent, casting conditions and surrounding environment are found to influence the

formation of BFs over PS [7]. Influence of the geometry of the PS polymer such as linear homopolymers [8, 9], rod-coil or coil-coil block copolymers [10], star-like homopolymers or copolymers [11] and amphiphilic polyion complexes [8] has been studied. Stenzel et al. [12] observed that only star shaped PS and PS with polar end groups resulted in BF formation while linear PS did not. But Peng et al., Bormashenko et al., Ferrari et al., reported the formation of BFs using linear PS [13–15]. Studies of PS [13–16] based BF formation have looked into the effect of molecular weight, the solvent used, substrate, atmospheric humidity on pore. Peng et al. [13] have used 1 wt.% PS of three molecular weights (29.3, 223.2 and 1970 K) on glass substrates with chloroform, toluene, carbon-di-sulfide (CS₂) and tetrahydrofuran (THF) as solvents. Ordered pores were obtained with toluene and chloroform at 60% relative humidity (RH) for molecular weight 223.2 K. The experiment was repeated using toluene varying the RH from 40 to 95% and ordered pores were obtained for RH varying from 46 to 90% with the pore size increasing with the increase in RH, while for RH greater than 90%, a polydispersion of the pore sizes was seen. Of the four solvents used, the evaporation rate of CS₂ and THF is higher than toluene and chloroform, in that case, the solvents CS₂ and THF completely evaporates before the water droplets form regular packing. While Ferrari et al.

^a e-mail: madhurima@cutn.ac.in (corresponding author)

Fig. 1 Schematic representation of the steps involved in BF formation



[15] used 1 wt.% PS of molecular weight 192 K in chloroform, CS_2 and dichloromethane to form breath figures on glass substrates at 75% RH. Only CS_2 could form ordered breath figures while chloroform resulted in random pores and dichloromethane with no pores. From the studies so far done, it is difficult to draw a conclusion regarding which solvent and under what conditions, BF formation is possible using PS. Bormashenko et al. [14] used different molecular weights of PS (4.8, 42.5, 227.1, 1000, 2800 K) in a mixture of chloroform (8 wt.%) with dichloromethane (92 wt.%) using 2.5 wt and 5 wt.% solutions under conditions of low humidity (30–40% RH). Bimodal distribution was obtained for molecular weights 4.8 and 42.5 K while at 227.1, 1000 K ordered pores were formed for both 2.5 and 5 wt.%. The 5 wt.% solution of 2800 K did not form a homogenous film while 2.5 wt.% of the same resulted in ordered BFs. Thus, PS is seen to form breath figures under various experimental conditions with no clarity regarding the influence of solvents, RH and molecular weight on the same. The orderliness of BFs over PS has been studied through image analysis involving the Voronoi entropy [17, 18] and fast Fourier transforms (FFT) [19]. Literature reports show that the wettability of the BF patterned surfaces is done and they showed hydrophobic nature [20, 21].

In an attempt to further understand the formation of BF on PS, this work reports the studies on the same for different molecular weights of PS and the influence of casting methods. Further, the influence of underlying symmetry of the substrate is also studied by casting the polymer on the smooth and the grooved surfaces of a commercial DVD, with the ordered grooves providing the necessary asymmetry. The images of the BFs formed under various conditions are analyzed in terms of Voronoi entropy and Fast Fourier Transforms. Contact angle studies of BF surfaces are done to investigate their wetting nature.

2 Methodology

2.1 Materials

PS of three molecular weights viz 35,000, 1,92,000 and 2,80,000 g/mol were purchased from *Sigma Aldrich*. Chloroform of purity 99.8% purchased from *Nice Chemicals (India)* was used as the solvent for the polymers. The smooth and grooved surfaces (cut into $1 \times 1 \text{ cm}^2$) of the commercially available Sony recordable DVD were used as substrates.

2.2 Experimental details

3 and 5 wt.% of the polymer solutions of the three polymers were prepared by dissolving 0.6 and 0.1 g in 2 ml of chloroform, respectively. A humid atmosphere was created by keeping 3 ml of distilled water in a petri-dish kept inside a closed chamber. 100 μl solution was drop-casted on the smooth and grooved surfaces and was kept in the humid atmosphere saturated with water vapor. The polymer solutions were spin-coated on the smooth and grooved DVD surfaces at 1000 rpm and were kept for pattern formation. The substrates after drying were imaged using the Leica Confocal Laser Scanning Microscope (CLSM) TCS SP8 model. The excitation wavelength of 633 nm was used to image the patterns formed. The diameter of the pores and the Voronoi entropy were calculated using the *ImageJ* software. Rame-Hart goniometer was used to measure the contact angle of water on various surfaces using staticsessile drop method. Figure 1 shows the experimental set up used for the BF experiment (Fig. 2).

3 Results and discussions

PS of three different molecular weights dissolved in chloroform (to make 3 and 5 wt.% solutions) up on

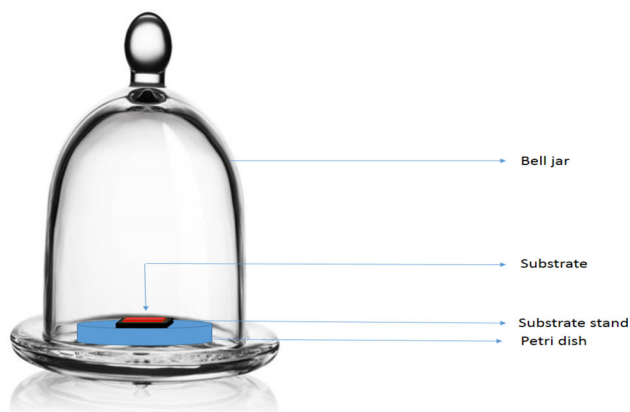


Fig. 2 Experimental set up used for BF formation

casting on the smooth and grooved surfaces of the DVD substrate were kept in a humid environment. To avoid the chances of uncertainty using the dynamic method of self-assembly, the static method of self-assembly is used for the pattern formation. After the complete evaporation of the solvent, confocal microscopy is used to observe the morphologies of the patterns obtained.

The patterns observed on smooth and grooved DVD surfaces on drop-casting and spin-coating using PS of three different molecular weights (35, 192, 280 K) using 3 and 5 wt.% solutions are shown in Tables 1, 2 and 3, respectively. Table 6 displays the histograms of the pore size distributions computed using the *ImageJ* software for the drop-casted samples. These histograms were fitted with a Gaussian curve [17] using Origin software and the mean diameter (MD) and standard deviation were obtained from them which is also tabulated in Table 6. On both smooth and grooved DVD surfaces during drop-casting, the pores observed were mostly circular in shape. For the same molecular weight and weight percentage, the pores on grooved surfaces are smaller than those on smooth surfaces on drop-casting. Also the pores on the grooved surfaces show a uniformity in size for all molecular weight and concentration when compared with the smooth. A similar study using polydimethylsiloxane (PDMS) did not show such a uniformity in pore size [22]. The likely reason for this could be because molecules of PS stack through π - π interactions and any small changes in their environment is known to disturb the same [23]. The underlying grooves on the substrate may disturb the π - π stacking causing water droplets condensation and evaporation easy and resulting in more ordered and uniform pores. A small molecular dynamics simulation of 3 styrene molecules was done to identify the π - π stacking in PS and the same is shown in Fig. 3 along with the chemical structure of PS.

The pore size of the BFs formed on drop-casted PS is found to increase with the increasing molecular weight and also with the weight percentage used. The effect of molecular weight [13, 14, 20, 24–26] and concentration [20, 27] of the polymer in pattern formation were previously studied by many research groups.

The polymer molecular weight and the concentration of polymer used are found to have a direct correlation on the pore size irrespective of the substrate used. Higher molecular weight leads to a higher vapor pressure which accelerates the rate of evaporation of the solvent, thus increasing the pore size [24]. Rapid evaporation results in a lower surface temperature, which enhances the water vapor condensation. Since large amounts of water droplets are condensing, coalescence can also occur resulting in larger pores eventually. The increase in pore size with the concentration is attributed to the increasing concentration lengthening the droplet growth period [14, 28, 29].

The surface morphology of the spin-coated and drop-casted patterns is different. Spin-coating of 3 and 5 wt.% of PS solutions on smooth surfaces gives random pores and the images were not amicable for further analysis. Also, pores were not observed on the grooved surface for 3 wt.% solutions of PS of all molecular weight and 5 wt.% solutions of molecular weight 35 K. Random pores were observed with 5 wt.% for molecular weights 192 and 280 K, respectively.

The near absence of breath figure patterns on spin-coated surfaces can be attributed to the thickness of the film. The thickness of the film during spin-coating depends on the viscosity of the polymer solution and the speed of rotation [30]. Here the speed of rotation is 1000 rpm, which is kept constant for all the spin-coated surfaces such that the thickness of the film depends on the viscosity of the solution. The viscosity of the polymer solution is related to molecular weight (M_v) by the semi-empirical Mark Houwink relation: $\eta = KM_v^\alpha$, where K and α are constants for a given polymer, solvent and temperature [31]. Also the viscosity of the solution is proportional to the concentration of the polymer solution [32]. Also it was previously experimentally observed that the thickness on spin-coating of a polymer solution for a particular spin velocity is directly proportional to both concentration and molecular weight [33]. Thus for 3 and 5 wt.% spin-coated samples, the thickness of the film may be insufficient to allow the formation of ordered BFs.

The length for long-range ordering is often limited in breath figures [34]. The FFT of CLSM (Tables 1, 2 and 3 has the FFT images for BFs formed) images shows a circular pattern which confirms multi-grain morphology and short range ordering. A similar multi-grain morphology has been reported in the BF formed using monocarboxy terminated PS, using FFT analysis [34].

Voronoi entropy (Shannon entropy) or Voronoi tessellation is a mathematical tool used for the quantification of the uniformity of the points arranged on a surface. Thus, this tool can be used to comment on the orderliness of the pores formed by the self-assembly process [35]. A Voronoi polygon is described as being the smallest convex polygon enclosing a point whose sides are perpendicular bisectors of the lines between a point and its neighbors. The number of sides ' n ' of the Voronoi polygon is known as the coordination number and P_n is the fraction of the polygon having the number of sides

Table 1 CLSM images, FFT, Voronoi tessellations and statistical analysis of polygons on Voronoi tessellations for molecular weight: 35 K on smooth and grooved DVD surfaces

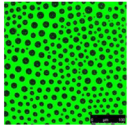
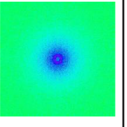
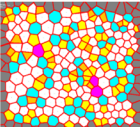
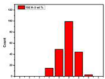

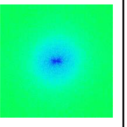
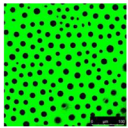
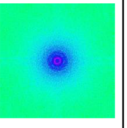
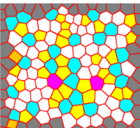
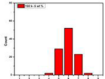
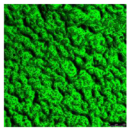
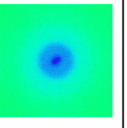
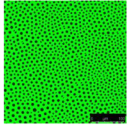
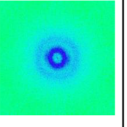
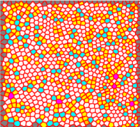
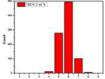
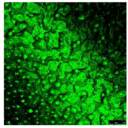
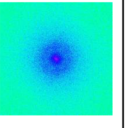
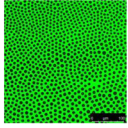
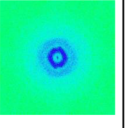
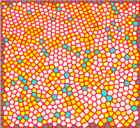
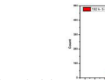
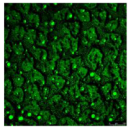
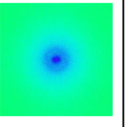
Surface	Weight percentage	Casting technique	CLSM images	FFT	Voronoi tessellations	Statistical analysis of polygons on Voronoi tessellations
Smooth	3	Drop-casting				S = 1.20
		Spin-coating			—	—
	5	Drop-casting				S = 1.21
		Spin-coating			—	—
Grooved	3	Drop-casting				S = 1.04
		Spin-coating			—	—
	5	Drop-casting				S = 1.06
		Spin-coating			—	—

‘*n*’. Using these values, a conformational entropy known as Voronoi entropy (*S*) is calculated using Eq. (1):

$$S = - \sum_n P_n \ln P_n \tag{1}$$

The summation is performed from *n* = 3 to the largest coordination number of any available polygon. The conformational entropy of the breath figure patterns are calculated and is compared with a perfectly hexagon pattern and completely random pattern whose entropy values are 0 and 1.71, respectively [36].

Table 2 CLSM images, FFT, Voronoi tessellations and statistical analysis of polygons on Voronoi tessellations for molecular weight: 192 K on smooth and grooved DVD surfaces

Surface	Weight percentage	Casting technique	CLSM images	FFT	Voronoi tessellations	Statistical analysis of polygons on Voronoi tessellations
Smooth	3	Drop-casting				S = 1.27 
		Spin-coating			—	—
	5	Drop-casting				S = 1.18 
		Spin-coating			—	—
Grooved	3	Drop-casting				S = 1.02 
		Spin-coating			—	—
	5	Drop-casting				S = 0.92 
		Spin-coating			—	—

The Voronoi entropy calculated for smooth and grooved surfaces for the three molecular weights are tabulated in Table 4.

The Voronoi tessellations of smooth and grooved surfaces for 35, 192 and 280 K are given in Tables 1, 2 and 3, respectively, along with the counts of the different polygons in the Voronoi diagram. The Voronoi entropy of BF's on grooved surfaces is less compared to that on smooth surfaces which indicates that the pores are

ordered on grooved surfaces. This uniformity in pore distribution is also seen from the confocal images of the BF's. The Voronoi entropies of smooth surfaces are much higher than the grooved surfaces and the most random distribution of pores is observed for PS with 280 K using 5 wt.% solution. This is also evident from the confocal image of the same.

There were studies based on the influence of the substrate surface energy on the pore ordering [15]. For the

Table 3 CLSM images, FFT, Voronoi tessellations and statistical analysis of polygons on Voronoi tessellations for molecular weight 280 K on smooth and grooved DVD surfaces

Surface	Weight percentage	Casting technique	CLSM images	FFT	Voronoi tessellations	Statistical analysis of polygons on Voronoi tessellations
Smooth	3	Drop-casting				S = 1.18
	5	Spin-coating			—	—
		Drop-casting				S = 1.36
		Spin-coating			—	—
Grooved	3	Drop-casting				S = 0.99
	5	Spin-coating			—	—
		Drop-casting				S = 1.05
		Spin-coating			—	—

PS/Chloroform solutions, substrates with higher surface energy formed long range ordering pores while for the PS/CS₂ solutions, substrates with the lower surface energy enabled the formation of ordered pores. Thus, from the literature, there are confusions regarding the contribution of the substrate to the ordering of the pores.

In addition to Voronoi entropy, Lewis law, Desch law and Aboav law can be used to study the topological properties of the Voronoi polygons of the BF patterned surfaces [37]. Lewis law relates the average area of n-sided polygon to the number of sides (*n*) by the relation (2)

Fig. 3 a: Chemical structure of PS, **b** π - π stacking in PS visualized using molecular dynamics

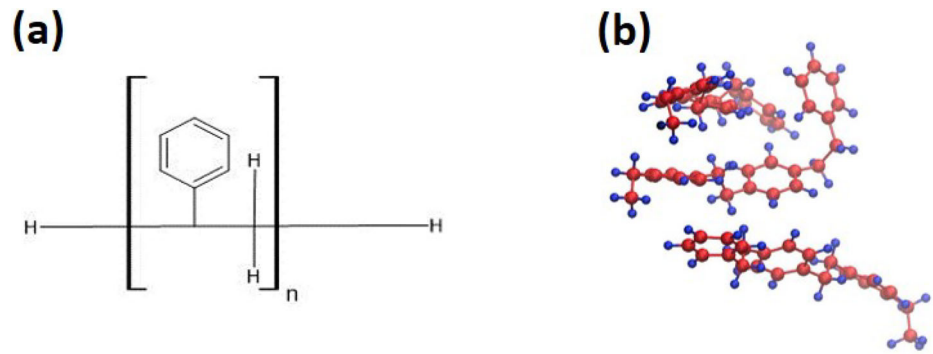


Table 4 Voronoi entropy for smooth and grooved surfaces along with the statistical scattering of polygons

Surfaces	Molecular weight and weight percentage	P_3	P_4	P_5	P_6	P_7	P_8	$S = -\sum_n P_n \ln P_n$
Smooth	35 K-3 wt.%	–	0.0225	0.297	0.463	0.193	0.0225	1.20
	35 K-5 wt.%	–	0.0509	0.325	0.451	0.164	0.0078	1.21
	192 K-3 wt.%	–	0.0714	0.233	0.471	0.209	0.0142	1.27
	192 K-5 wt.%	–	0.0185	0.268	0.481	0.212	0.0185	1.18
	280 K-3 wt.%	0.006	0.019	0.282	0.50	0.192	0.0128	1.18
	280 K-5 wt.%	–	0.094	0.235	0.458	0.164	0.047	1.36
Grooved	35 K-3 wt.%	–	0.0155	0.345	0.518	0.118	0.0021	1.04
	35 K-5 wt.%	–	0.0185	0.348	0.510	0.117	0.0055	1.06
	192 K-3 wt.%	–	0.012	0.312	0.555	0.113	0.0056	1.02
	192 K-5 wt.%	–	0.0114	0.363	0.558	0.0664	–	0.92
	280 K-3 wt.%	–	0.0052	0.281	0.568	0.142	0.0026	0.99
	280 K-5 wt.%	–	0.008	0.298	0.526	0.163	0.0028	1.05

$$A_n = \alpha(n - 2) \tag{2}$$

where α is the proportionality constant, i.e., a linear relationship exist between the average area of n -polygon and n . The analysis of Voronoi polygons of BF patterned surfaces using Lewis Law is shown in Fig. 4.

Desch law states that there exists a linear relationship between the perimeter of the polygon and the number of their sides. Figure 5 shows the analysis of Voronoi polygons of BF patterned surface using Desch law.

Aboavs law states that the average number of sides (m_n) surrounding a n -sided polygon varies linearly with $1/n$. The law is usually written in the form of Eq. (3):

$$m_n = a + \frac{b}{n} \tag{3}$$

where a and b are constants. Figure 6 shows the analysis of Voronoi polygons of BF patterned surfaces using Aboavs law.

Table 5 summarizes the fitting parameter R^2 value obtained during the linear fitting for the three laws. The Aboav's law is well verified with the experimental data with the R^2 value in the range 0.96–0.99 for both smooth and grooved surfaces. The Lewis law also shows a good fitting with the R^2 value \geq 0.91 except for

PS 35 K 5 wt.% smooth, and on grooved 192 K-3 and 5 wt.% and 280 K-5 wt.%. The linear fitting of Desch law is also good with R^2 value 0.921–0.987 except for a few. It was observed in literature that Lewis law and Desch law does not hold good for monodisperse compact packing with packing fraction of 0.45 or greater than 0.45 due to steric exclusion which gives high values of area and perimeter for lower order polygons [38] (Fig. 7) (Table 6).

3.1 Wettability studies

The wettability of a solid surface by a liquid is quantified the Young's equation (Eq. 4), which is a relation between the solid–liquid interfacial tension (γ_{SL}), solid–vapor interfacial tension (γ_{SG}) and liquid vapor–interfacial tension (γ_{LG}) comes into action and the contact angle (θ_c) formed at the triple phase contact line [39].

$$\cos \theta_c = \frac{\gamma_{SG} - \gamma_{SL}}{\gamma_{LG}} \tag{4}$$

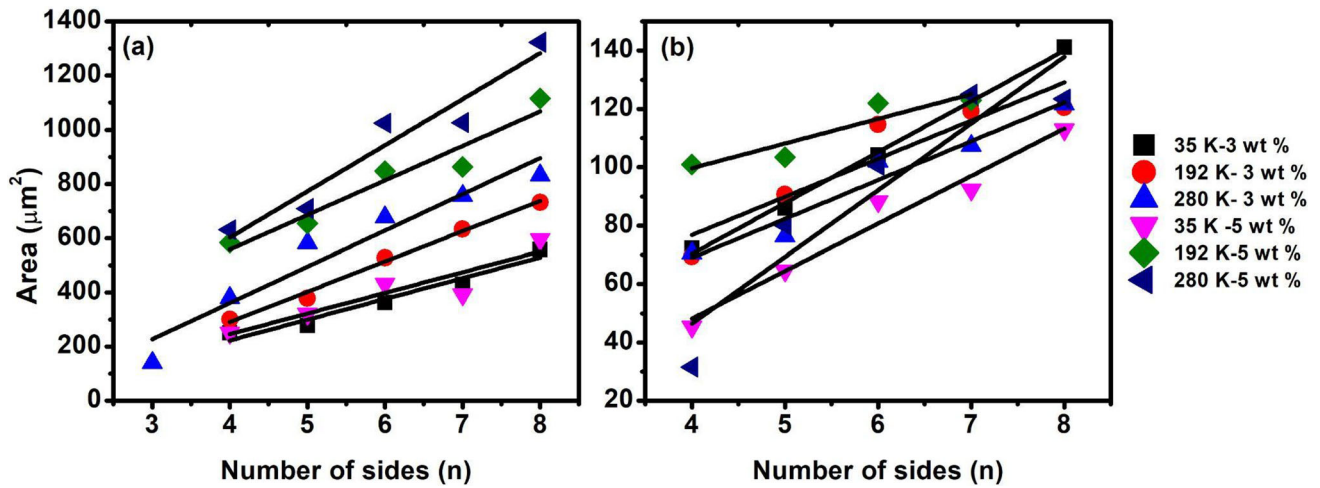


Fig. 4 Area of polygon versus the number of sides a: Smooth; b: Grooved

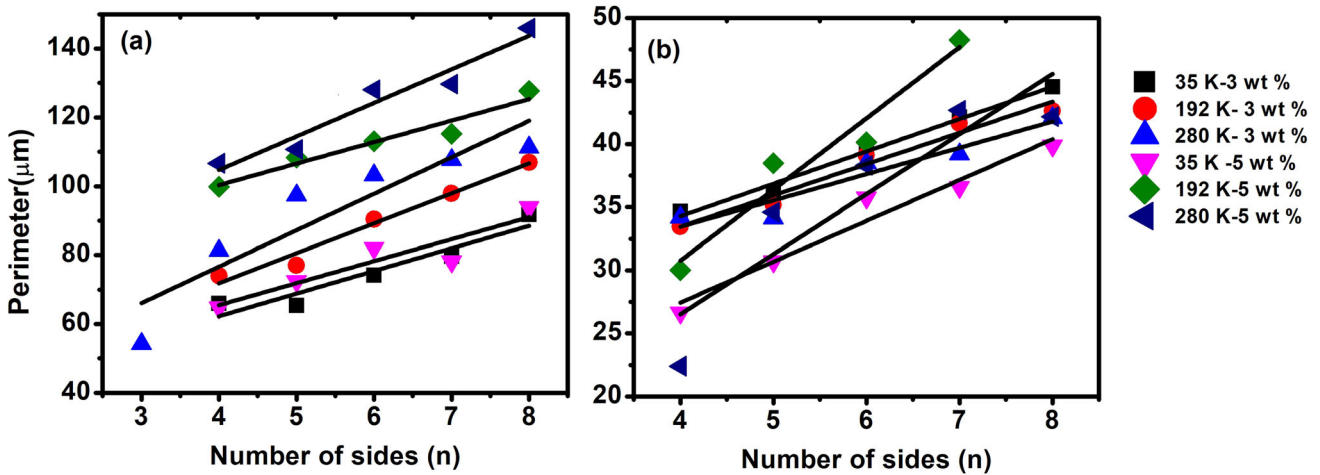


Fig. 5 Perimeter of polygon versus the number of sides a: Smooth; b: Grooved

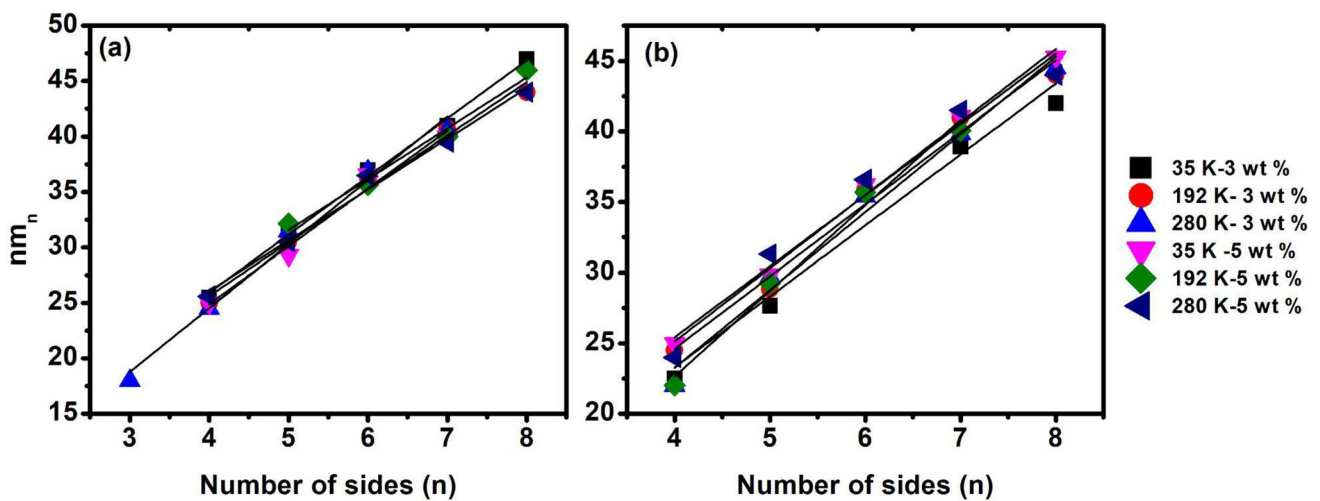
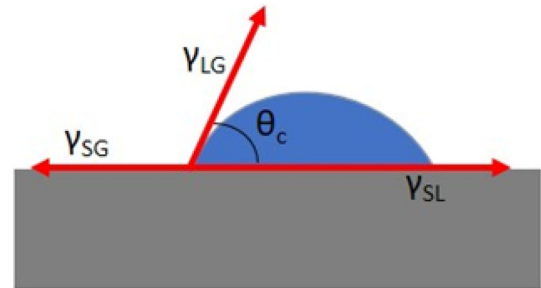


Fig. 6 Aboavs Law for a: Smooth; b: Grooved

Table 5 The fitting parameter R^2 value obtained during the linear fitting for the three laws

Laws	Smooth						Grooved					
	35 K		192 K		280 K		35 K		192 K		280 K	
	3 wt.%	5 wt.%	3 wt.%	5 wt.%	3 wt.%	5 wt.%	3 wt.%	5 wt.%	3 wt.%	5 wt.%	3 wt.%	5 wt.%
Lewis	0.939	0.808	0.990	0.914	0.918	0.911	0.996	0.957	0.814	0.793	0.941	0.838
Desch	0.880	0.815	0.967	0.922	0.808	0.925	0.987	0.944	0.955	0.921	0.897	0.768
Aboavs	0.994	0.973	0.986	0.976	0.983	0.988	0.956	0.993	0.979	0.982	0.981	0.962

Fig. 7 Schematic representation of a water droplet on solid surface showing the quantities in Youngs equation



Wettability studies of the drop-casted and spin-coated surfaces were done taking water as the test liquid using the contact angle measurements. The results, Fig. 8, indicate that the contact angle over spin-coated surfaces is lesser than over drop-casted surfaces which is because of the formation of BFs on the drop-casted surfaces. A flat PS film has a water contact angle of 89° [40]. It is known that highly porous films may entrap air and remain in the Cassie state [41]. The apparent contact angles can be calculated using the Cassie and Baxter’s law [40] (Eq. 5):

$$\cos \theta_{\text{calc}} = (1 - f_{\text{pores}}) * \cos \theta_{\text{polymer}} + \cos \theta_{\text{pore}} * f_{\text{pores}} \tag{5}$$

where θ_{calc} is the calculated contact angle; f_{pores} -area fraction of pores; θ_{polymer} -contact angle of the polymer; θ_{pore} - contact angle of the pore in the Cassie state (180°).

The area fraction of pores are calculated from the confocal images and the calculated contact angle values using Cassie and Baxters law are found to be close to the experimental values which are tabulated below

(Table 7). These data confirm the Cassie-Baxter state of wetting of the BF patterned surfaces. The increased hydrophobicity of the BF patterned surfaces may be useful for the fabrication of water repellent surfaces.

4 Conclusions

The formation of porous polymer film on PS using BF method on smooth and grooved surfaces of the DVD substrate is reported. It is observed that the variation of the molecular weight affects the size of the pores formed. The pore diameters increase with the increasing molecular weight and concentration. On grooved surfaces, a near uniformity of pore diameters is observed, probably due to the disruption of the PS stacking. Voronoi entropy confirms that more ordered pores are formed on grooved surfaces compared to the smooth ones. Wetting studies show the patterned BF surfaces to be hydrophobic, with the hydrophobicity increasing with an increase in the asymmetry of the underlying substrates, namely the grooves.

Table 6 Histogram of the pore size distribution on smooth and grooved surfaces using different molecular weights of PS during drop-casting

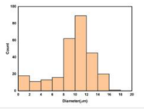
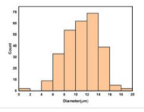
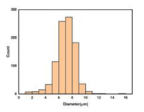
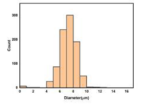
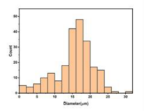
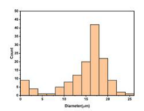
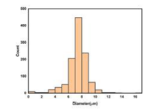
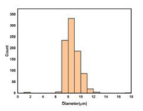
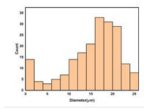
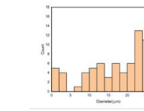
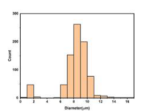
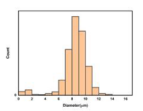
Molecular weight	Smooth		Grooved	
	3 wt.%	5 wt.%	3 wt.%	5 wt.%
35 K	 M.D: 10.72 ± 0.15	 M.D: 11.31 ± 0.24	 MD: 7.17 ± 0.03	 M D: 7.37 ± 0.02
192 K	 M.D: 16.78 ± 0.24	 M D: 17.04 ± 0.19	 M D: 7.55 ± 0.02	 M D: 8.48 ± 0.06
280 K	 M D: 18.03 ± 0.42	 M D: 25.80 ± 0.54	 M D: 8.67 ± 0.05	 M D: 8.74 ± 0.02

Fig. 8 Contact angle values for drop-casted and spin-coated smooth and grooved surfaces using 3 and 5 wt.% PS solutions

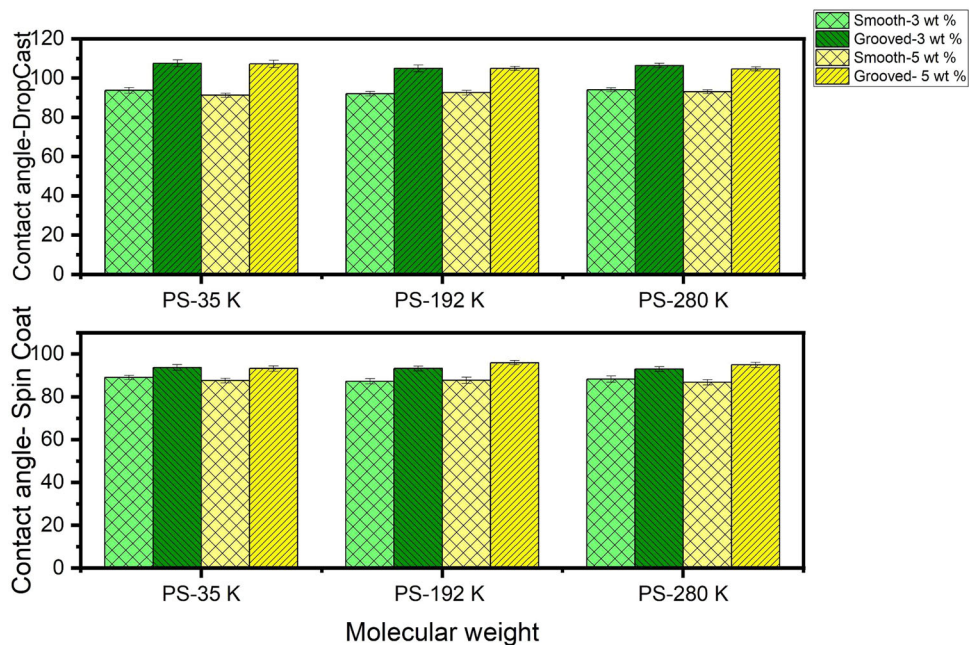


Table 7 Contact angle values calculated for drop casted surfaces using the Cassie-Baxter law

Molecular weight	Smooth		Grooved	
	3 wt.%	5 wt.%	3 wt.%	5 wt.%
35 K	98.3	100	105.5	109.79
192 K	102	99.5	105.5	112
280 K	103	102	108.5	104.3

Acknowledgements Swathi P V acknowledges DST, Govt. of India for the Inspire Fellowship (IF190317). The authors acknowledge S G Ramkumar for giving the idea of spin-coating. The authors acknowledge Chandra Mouli P V S S R for the discussions on image analysis. The authors acknowledge Abdulkareem U for running the MD simulation of PS. The authors thank the Naval Research Board of India for the contact angle goniometer.

Author contribution statement

VM conceived the original idea. SPV performed the experiments. Both the authors were involved equally in the analysis of the results and writing the manuscript.

Data availability The datasets generated and/or analyzed during the current study are available from the corresponding author on reasonable request.

Declarations

Conflict of interest The authors declare no conflict of interest.

References

- P.T. Tanev, M. Chibwe, T.J. Pinnavaia, Titanium-containing mesoporous molecular sieves for catalytic oxidation of aromatic compounds. *Nature* **368**, 321–323 (1994). <https://doi.org/10.1038/368321a0>
- H. Deleuze, X. Schultze, D.C. Sherrington, Polymer-supported titanates as catalysts for transesterification reactions. *Polymer* **39**, 6109–6114 (1998). [https://doi.org/10.1016/S0032-3861\(98\)00080-9](https://doi.org/10.1016/S0032-3861(98)00080-9)
- K. Lewandowski, P. Murer, F. Svec, J.M.J. Fréchet, The design of chiral separation media using monodisperse functionalized macroporous beads: effects of polymer matrix, tether, and linkage chemistry. *Anal. Chem.* **70**, 1629–1638 (1998). <https://doi.org/10.1021/ac971196x>
- D.B. Akolekar, A.R. Hind, S.K. Bhargava, Synthesis of macro-, meso-, and microporous carbons from natural and synthetic sources, and their application as adsorbents for the removal of quaternary ammonium compounds from aqueous solution. *J. Colloid Interface Sci.* **199**, 92–98 (1998). <https://doi.org/10.1006/jcis.1997.5352>
- S. Xie, F. Svec, J.M.J. Fréchet, Rigid porous polyacrylamide-based monolithic columns containing butyl methacrylate as a separation medium for the rapid hydrophobic interaction chromatography of proteins. *J. Chromatogr. A* **775**, 65–72 (1997). [https://doi.org/10.1016/S0021-9673\(97\)00254-9](https://doi.org/10.1016/S0021-9673(97)00254-9)
- B. François, O. Pitois, J. François, Polymer films with a self-organized honeycomb morphology. *Adv. Mater.* **7**, 1041–1044 (1995). <https://doi.org/10.1002/adma.19950071217>
- H. Yabu, Fabrication of honeycomb films by the breath figure technique and their applications. *Sci. Technol. Adv. Mater.* **19**, 802–822 (2018). <https://doi.org/10.1080/14686996.2018.1528478>
- O. Karthaus, N. Maruyama, X. Cieren, M. Shimomura, H. Hasegawa, T. Hashimoto, Water-assisted formation of micrometer-size honeycomb patterns of polymers. *Langmuir* **16**, 6071–6076 (2000). <https://doi.org/10.1021/la0001732>
- M. Srinivasarao, D. Collings, A. Philips, S. Patel, Three-dimensionally ordered array of air bubbles in a polymer film. *Science* **292**, 79–83 (2001). <https://doi.org/10.1126/science.1057887>
- B. de Boer, U. Stalmach, H. Nijland, G. Hadziioannou, Microporous honeycomb-structured films of semiconducting block copolymers and their use as patterned templates. *Adv. Mater.* **12**, 1581–1583 (2000). [https://doi.org/10.1002/1521-4095\(200011\)12:21%3c1581::AID-ADMA1581%3e3.0.CO;2-R](https://doi.org/10.1002/1521-4095(200011)12:21%3c1581::AID-ADMA1581%3e3.0.CO;2-R)
- G. Widawski, M. Rawiso, B. François, Self-organized honeycomb morphology of star-polymer polystyrene films. *Nature* **369**, 387–389 (1994). <https://doi.org/10.1038/369387a0>
- M.H. Stenzel-Rosenbaum, T.P. Davis, A.G. Fane, V. Chen, Porous polymer films and honeycomb structures made by the self-organization of well-defined macromolecular structures created by living radical polymerization techniques. *Angew. Chem. Int. Ed.* **40**, 3428–3432 (2001). [https://doi.org/10.1002/1521-3773\(20010917\)40:18%3c3428::AID-ANIE3428%3e3.0.CO;2-6](https://doi.org/10.1002/1521-3773(20010917)40:18%3c3428::AID-ANIE3428%3e3.0.CO;2-6)
- J. Peng, Y. Han, Y. Yang, B. Li, The influencing factors on the macroporous formation in polymer films by water droplet templating. *Polymer* **45**, 447–452 (2004). <https://doi.org/10.1016/j.polymer.2003.11.019>
- E. Bormashenko, R. Pogreb, O. Stanevsky, Y. Bormashenko, O. Gendelman, Formation of honeycomb patterns in evaporated polymer solutions: influence of the molecular weight. *Mater. Lett.* **59**, 3553–3557 (2005). <https://doi.org/10.1016/j.matlet.2005.06.026>
- E. Ferrari, P. Fabbri, F. Pilati, Solvent and substrate contributions to the formation of breath figure patterns in polystyrene films. *Langmuir* **27**, 1874–1881 (2011). <https://doi.org/10.1021/la104500j>
- M.H. Stenzel, C. Barner-Kowollik, T.P. Davis, Formation of honeycomb-structured, porous films via breath

- figures with different polymer architectures. *J. Polym. Sci. Part Polym. Chem.* **44**, 2363–2375 (2006). <https://doi.org/10.1002/pola.21334>
17. L. Ruiz-Rubio, I. Azpitarte, N. García-Huete, J.M. Laza, J.L. Vilas, L.M. León, Solvent and relative humidity effect on highly ordered polystyrene honeycomb patterns analyzed by Voronoi tessellation. *J. Appl. Polym. Sci.* (2016). <https://doi.org/10.1002/app.44004>
 18. A.V. Limaye, R.D. Narhe, A.M. Dhote, S.B. Ogale, Evidence for convective effects in breath figure formation on volatile fluid surfaces. *Phys. Rev. Lett.* **76**, 3762–3765 (1996). <https://doi.org/10.1103/PhysRevLett.76.3762>
 19. B.-H. Wu, L.-W. Wu, K. Gao, S.-H. Chen, Z.-K. Xu, L.-S. Wan, Self-assembly of patterned porous films from cyclic polystyrenes via the breath figure method. *J. Phys. Chem. C* **122**, 3926–3933 (2018). <https://doi.org/10.1021/acs.jpcc.7b12286>
 20. W. Dong, Y. Zhou, D. Yan, Y. Mai, L. He, C. Jin, Honeycomb-structured microporous films made from hyperbranched polymers by the breath figure method. *Langmuir* **25**, 173–178 (2009). <https://doi.org/10.1021/la802863m>
 21. S. Zhai, J.-R. Ye, N. Wang, L.-H. Jiang, Q. Shen, Fabrication of porous film with controlled pore size and wettability by electric breath figure method. *J Mater Chem C* **2**, 7168–7172 (2014). <https://doi.org/10.1039/C4TC01271B>
 22. K. Nilavarasi, V. Madhurima, Controlling breath figure patterns on PDMS by concentration variation of ethanol-methanol binary vapors. *Eur. Phys. J. E.* **41**, 82 (2018). <https://doi.org/10.1140/epje/i2018-11691-x>
 23. W. Cai, D. Xu, L. Qian, J. Wei, C. Xiao, L. Qian, Z. Lu, S. Cui, Force-induced transition of π - π stacking in a single polystyrene chain. *J. Am. Chem. Soc.* **141**, 9500–9503 (2019). <https://doi.org/10.1021/jacs.9b03490>
 24. Y. Xu, B. Zhu, Y. Xu, A study on formation of regular honeycomb pattern in polysulfone film. *Polymer* **46**, 713–717 (2005). <https://doi.org/10.1016/j.polymer.2004.12.001>
 25. A.M. Rawlett, J.A. Orlicki, N. Zander, A. Karikari, T. Long, T, Self assembled, ultra-hydrophobic micro/nano-textured surfaces. Army Research Lab Aberdeen Proving Ground MD Weapons and Materials Research (2007)
 26. H. Matsuyama, K. Ohga, T. Maki, M. Teramoto, The effect of polymer molecular weight on the structure of a honeycomb patterned thin film prepared by solvent evaporation. *J. Chem. Eng. Jpn.* **37**, 588–591 (2004). <https://doi.org/10.1252/jcej.37.588>
 27. B. Zhao, C. Li, Y. Lu, X. Wang, Z. Liu, J. Zhang, Formation of ordered macroporous membranes from random copolymers by the breath figure method. *Polymer* **46**, 9508–9513 (2005). <https://doi.org/10.1016/j.polymer.2005.07.035>
 28. Y. Zhu, R. Sheng, T. Luo, H. Li, J. Sun, S. Chen, W. Sun, A. Cao, Honeycomb-structured films by multi-functional amphiphilic biodegradable copolymers: surface morphology control and biomedical application as scaffolds for cell growth. *ACS Appl. Mater. Interfaces* **3**, 2487–2495 (2011)
 29. H. Li, Y. Jia, M. Du, J. Fei, J. Zhao, Y. Cui, J. Li, Self-organization of honeycomb-like porous TiO₂ films by means of the breath-figure method for surface modification of titanium implants. *Chem. Eur. J.* **19**, 5306–5313 (2013). <https://doi.org/10.1002/chem.201203353>
 30. B.S. Yilbas, A. Al-Sharafi, H. Ali, Surfaces for Self-Cleaning, in *Self-Cleaning of Surfaces and Water Droplet Mobility*. (Elsevier, 2019), pp.45–98
 31. P.J. Flory, *Principles of Polymer Chemistry* (Cornell University Press, 1953)
 32. Y. Hong, Electrospun Fibrous Polyurethane Scaffolds in Tissue Engineering, in *Advances in Polyurethane Biomaterials*. (Elsevier, 2016), pp.543–559
 33. D.W. Schubert, Spin coating as a method for polymer molecular weight determination. *Polym. Bull.* **38**, 177–184 (1997). <https://doi.org/10.1007/s002890050035>
 34. J.S. Park, S.H. Lee, T.H. Han, S.O. Kim, Hierarchically ordered polymer films by templated organization of aqueous droplets. *Adv. Funct. Mater.* **17**, 2315–2320 (2007). <https://doi.org/10.1002/adfm.200601141>
 35. C.M. Knobler, D. Beysens, Growth of breath figures on fluid surfaces. *Europhys. Lett.* **6**, 707–712 (1988). <https://doi.org/10.1209/0295-5075/6/8/007>
 36. A. Muñoz-Bonilla, M. Fernández-García, J. Rodríguez-Hernández, Towards hierarchically ordered functional porous polymeric surfaces prepared by the breath figures approach. *Prog. Polym. Sci.* **39**, 510–554 (2014). <https://doi.org/10.1016/j.progpolymsci.2013.08.006>
 37. E. Bormashenko, M. Frenkel, A. Vilik, I. Legchenkova, A. Fedorets, N. Aktaev, L. Dombrovsky, M. Nosonovsky, Characterization of self-assembled 2D patterns with voronoi entropy. *Entropy* **20**, 956 (2018). <https://doi.org/10.3390/e20120956>
 38. C. Annic, J.P. Troadec, A. Gervois, J. Lemaître, M. Ammi, L. Oger, Experimental study of radical tessellations of assemblies of discs with size distribution. *J. Phys. I(4)*, 115–125 (1994). <https://doi.org/10.1051/jp1:1994124>
 39. T. Young, III. An essay on the cohesion of fluids. *Philos. Trans. R. Soc. Lond.* **95**, 65–87 (1805). <https://doi.org/10.1098/rstl.1805.0005>
 40. B.-B. Ke, L.-S. Wan, Y. Li, M.-Y. Xu, Z.-K. Xu, Selective layer-by-layer self-assembly on patterned porous films modulated by Cassie-Wenzel transition. *Phys. Chem. Chem. Phys.* **13**, 4881–4887 (2011). <https://doi.org/10.1039/C0CP01229G>
 41. E. Bormashenko, Y. Bormashenko, G. Whyman, R. Pogreb, O. Stanevsky, Micrometrically scaled textured metallic hydrophobic interfaces validate the Cassie-Baxter wetting hypothesis. *J. Colloid Interface Sci.* **302**, 308–311 (2006). <https://doi.org/10.1016/j.jcis.2006.06.016>

Springer Nature or its licensor (e.g. a society or other partner) holds exclusive rights to this article under a publishing agreement with the author(s) or other rightsholder(s); author self-archiving of the accepted manuscript version of this article is solely governed by the terms of such publishing agreement and applicable law.